JOURNAL OF PETROLEUM GEOMECHANICS
(JPG)

Original article

Investigating the Ground Deformation During and After CO_2 Sequestration in Deep Saline Aquifers

Mohammad Ali Iranmanesh[1*]

1- Assistant Professor, Civil Engineering Faculty, K. N. Toosi University of Technology, Tehran, Iran

Received: 29 April 2024; Accepted: 10 August 2024

DOI: 10.22107/jpg.2024.485964.1243

Keywords

CO_2 Sequestration,
Saline Aquifers,
Ground Deformation,
Numerical Analysis,
Anisotropic Permeability

Abstract

CO_2 injection in saline aquifers is a crucial method for carbon sequestration, reducing atmospheric CO_2 levels and mitigating climate change. Saline aquifers, due to their large capacity and widespread availability, serve as effective storage sites for CO_2, helping to isolate it long-term and prevent its release back into the atmosphere. This study investigates the uplift of the top surface of a deep saline aquifer due to CO_2 injection, using the finite element numerical approach. The density and viscosity of the injected supercritical CO_2 were considered as functions of temperature and pressure, while the density and viscosity of saline water were similarly modeled as temperature- and pressure-dependent. Geothermal temperature variations were also incorporated into the model. Additionally, the effects of halting injection after a certain period and the subsequent spread of injected CO_2 in the aquifer, driven by capillary and gravitational forces, were examined in relation to the displacements. Both horizontal and vertical well configurations were studied. The modeling results indicated that with a vertical well, the CO_2 plume extended to higher levels and farther distances from the injection point compared to a horizontal well, resulting in greater surface uplift with the horizontal well configuration. The impact of permeability anisotropy was also analyzed, revealing that when horizontal permeability is ten times greater than vertical permeability, the CO_2 plume spreads horizontally, substantially reducing the aquifer surface uplift.

1. Introduction

With the increasing concentration of greenhouse gases in the atmosphere, particularly carbon dioxide (CO_2), global warming and climate change have become one of the most significant environmental challenges of the 21st century. Carbon dioxide, as the primary greenhouse gas, plays a prominent role in raising global temperatures, and controlling its emissions has become one of the key objectives of scientific and industrial communities. One promising solution for reducing CO_2 concentrations in the atmosphere is Carbon Capture and Storage (CCS) technologies [1,2]. These technologies enable the capture of carbon dioxide from emission sources such as fossil fuel power plants and heavy industries, followed by its safe storage underground.

Among these methods, the sequestration of carbon dioxide in saline aquifers has emerged as one of the most attractive options [3,4]. Saline reservoirs, which consist of porous rocks containing salty water deep underground, are considered suitable for this process due to their large capacity, geographical extent, and ability to provide long-term storage of CO_2 [5]. In this method, CO_2 is injected in a compressed state and under pressure into the reservoirs, where it interacts with the porous rocks and saline water, resulting in its mechanical, solution, and mineral trapping.

While this method is considered a promising

* Civil Engineering Faculty, K. N. Toosi University of Technology, Valiasr Street, Mirdamad Intersection, Tehran, Iran. Email: Iranmanesh@kntu.ac.ir

approach for mitigating climate change, it can cause several geological consequences, especially ground deformations. When CO_2 is injected into a deep saline aquifer, it displaces the brine, leading to a significant increase in pore pressure in the reservoir. This increase in pressure can cause the rock matrix to expand and result in surface uplift. The degree of uplift depends on factors such as the volume of CO_2 injected, the depth and thickness of the aquifer, the rock's mechanical properties, and the permeability of the surrounding formations. Although surface uplift is generally small (on the order of millimeters to a few centimeters), it could be problematic in areas with sensitive infrastructure [6,7]. For instance, injection-induced uplift has been observed in some sequestration projects, such as the In Salah Project in Algeria, where satellite measurements recorded an uplift of a few millimeters per year [8,9]. The injection of CO_2 into a saline aquifer can also deform the overlying caprock, which is critical for trapping the CO_2 and preventing it from migrating to the surface. If the caprock fractures due to stress changes from the injection, it could create leakage pathways for CO_2 to escape, compromising the storage integrity [10]. Furthermore, increased pore pressure from CO_2 injection can reduce the effective normal stress on pre-existing faults, potentially causing them to slip and reactivate. This process, known as injection-induced seismicity, can lead to small to moderate earthquakes. If a fault slip occurs near the surface, it can result in localized ground deformations [11,12]. The mechanical properties of the reservoir rock (elasticity and compressibility), as well as the aquifer's porosity and permeability, strongly influence the extent of ground deformation. The total volume of CO_2 injected, and the rate of injection are major factors. Higher volumes and pressures increase the likelihood of deformation [13].

Once injection is stopped, the pore pressure in the aquifer may gradually decrease over time as CO_2 diffuses throughout the reservoir. This can lead to long-term settling or re-equilibration of ground deformation, reducing the immediate effects of uplift or subsidence.

Numerous studies have been conducted on various aspects of CO_2 sequestration in saline aquifers. Including fieldwork and laboratory experiments [14,15], as well as analytical, and numerical investigations [8,16–19].

In this study, the ground deformation during and after carbon dioxide injection in an anisotropic saline aquifer is investigated through the numerical finite element method. Throughout the paper, ground displacement refers specifically to the displacement of the upper surface of the aquifer. In this study, the primary focus is on quantifying the displacement of the aquifer's upper surface. This displacement may extend to the ground surface, which is significant as it could lead to fractures in the caprock, potentially compromising its integrity. The term "anisotropy" refers to anisotropy in intrinsic permeability. The injection is assumed to occur at a constant rate for a specific period, followed by the spreading and diffusion of CO_2 through the aquifer due to gravity and capillary forces. The effects of pressure and temperature on the density and dynamic viscosity of brine and supercritical CO_2 are also considered. Additionally, the ground deformation profile is examined for both horizontal and vertical injection wells. It is worth noting that the numerical simulations were performed using the commercial software COMSOL Multiphysics, which is based on the finite element method.

In the following, first the equations governing the flow of two immiscible fluids through porous media along with the solid deformation are presented. This is followed by the problem definition and key assumptions. The numerical results and discussions are then presented, and the paper concludes with final remarks.

2. Formulation

The process of injecting carbon dioxide into a saline aquifer involves the flow of two immiscible fluids: brine and CO_2. Additionally, the deformation of the solid matrix must be considered to analyze the ground deformation induced by CO_2 injection. Therefore, the following equations govern this phenomenon [20].

(i) The linear momentum balance equation for the whole mixture:

$$\boldsymbol{\sigma}_{ij,j} + \rho \mathbf{g}_i = 0 \tag{1}$$

(ii) The mass conservation equation for each fluid phase:

$$\frac{\partial}{\partial t}\left(n s_\pi \rho_\pi\right) + \nabla\left(n \rho_\pi s_\pi \dot{\mathbf{u}}_i^\pi\right) = Q_\pi \tag{2}$$

(iii) The mass conservation equation for solid phase:

$$\frac{\partial}{\partial t}\left[(1-n)\rho_s\right]+\nabla\left[(1-n)\rho_s\dot{\mathbf{u}}_i\right]=0 \quad (3)$$

(iv) The extended Darcy's law:

$$ns_\pi\dot{\mathbf{u}}_i^\pi=\frac{\mathbf{K}_{ij}k_{r\pi}}{\mu_\pi}\left(-p_{\pi,j}+\rho_\pi\mathbf{g}_j\right) \quad (4)$$

Where $\boldsymbol{\sigma}_{ij}$ is the total stress tensor, ρ is the average density of the mixture, ρ_s is the solid phase density, and n denotes the porosity. The subscript π stands for w or nw which represents wetting and non-wetting fluids. Therefore, s_π, ρ_π, μ_π, and p_π denote the degree of saturation, density, dynamic viscosity, and pressure for fluid phases, respectively. $\mathbf{g}_i$ is the gravity acceleration vector and Q_π denotes the fluid mass source or sink. $\mathbf{K}_{ij}$ is the intrinsic permeability tensor and $k_{r\pi}$ is the relative permeability coefficient of each fluid phase. $\dot{\mathbf{u}}_i$ and $\dot{\mathbf{u}}_i^\pi$ are the solid phase and fluid phase velocity vectors, respectively. In addition, the relationship between the degrees of fluid saturations can be written as:

$$s_w+s_{nw}=1 \quad (5)$$

The pore fluid pressures are related to each other via capillary pressure (p_c) as:

$$p_c=p_{nw}-p_w \quad (6)$$

The relationships between wetting-phase saturation and capillary pressure, as well as between saturations and relative permeabilities, are described using empirical functions:

$$\begin{aligned} s_w&=f(p_c)\\ k_{r\pi}&=f(s_\pi)\end{aligned} \quad (7)$$

In this study, experimental relations proposed by Brooks and Corey [21,22] are exploited to describe the saturation-capillary pressure and saturation-relative permeabilities equations:

$$\begin{aligned} s_e&=(s_w-s_{wr})/(1-s_{wr})\\ p_c&=p_b s_e^{(-1/\lambda)}\\ k_{rw}&=s_e^{(2+3\lambda)/\lambda}\\ k_{rnw}&=(1-s_e)^2(1-s_e^{(2+\lambda)/\lambda})\end{aligned} \quad (8)$$

Where s_e is the effective wetting phase saturation, s_{wr} is the residual wetting phase saturation, λ is the pore size distribution index and p_b is the bubbling pressure.

The relationship between the stress tensor and pore pressures is governed by Terzaghi's well-known effective stress principle, as follows:

$$\boldsymbol{\sigma}''_{ij}=\boldsymbol{\sigma}_{ij}+\alpha p\boldsymbol{\delta}_{ij} \quad (9)$$

Where $\boldsymbol{\sigma}''_{ij}$ is the effective stress tensor, α is the Biot's parameter, p is the average pore pressure and $\boldsymbol{\delta}_{ij}$ is the Kronecker delta.

3. Problem Definition and assumptions

To examine the impact of CO_2 injection on ground deformation, a part of a saline aquifer with dimensions of 5000 meters by 5000 meters and a constant thickness of 300 meters at a depth of 3000 meters from the surface is considered. The aquifer's upper boundary is located 2700 meters below the ground surface. In the center of the aquifer, an injection well introduces CO_2 into the reservoir over a length of 100 meters at a constant rate.

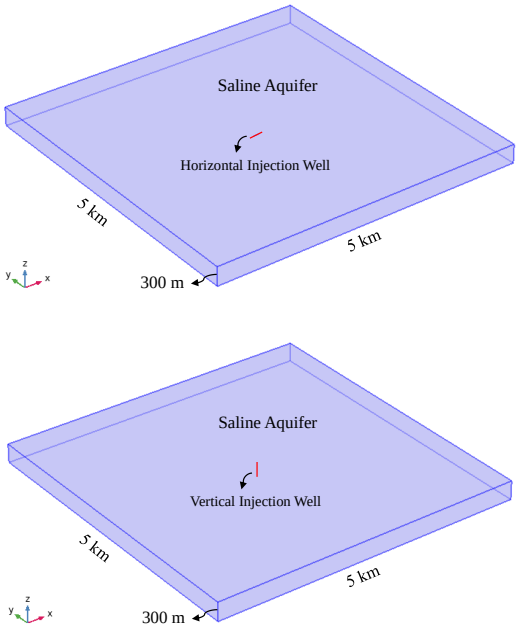

Fig. 1. Geometry of the saline aquifer along with the location of horizontal and vertical wells.

Both horizontal and vertical well configurations are modeled, allowing for an assessment of how well orientation affects the parameters under study. Fig. 1 illustrates the aquifer geometry and the location of the injection wells in both vertical and horizontal configurations. It should be noted that the vertical well is aligned along the z-axis, while the horizontal well is oriented along the x-

axis.The initial CO_2 saturation and hydraulic head are assumed to be zero across the entire aquifer. Boundary conditions are set such that CO_2 saturation and hydraulic head are also zero along the lateral boundaries. The top and bottom boundaries are considered impervious. Additionally, a boundary load equivalent to the effective weight of the overlying caprock is applied at the top boundary of the aquifer. The lateral boundaries are constrained in the horizontal directions, while the bottom boundary is fixed against displacement in all directions. Temperature variations with depth are also considered, with a temperature of 100°C assumed at a depth of 3000 meters, decreasing by 0.03°C per meter toward the surface.

The model incorporates the effects of pressure and temperature on the viscosity and density of saline water. Additionally, variations in the density of supercritical CO_2 with temperature and pressure are accounted by using the Peng-Robinson equation of state, and the Brokaw model is applied to capture changes in the viscosity of supercritical CO_2 [23]. The Peng-Robinson equation of state (PR EOS) is a widely used thermodynamic model for describing the behavior of fluids, particularly in petroleum and chemical engineering. It is commonly applied to predict the properties of gases and liquids under varying pressure and temperature conditions. It is used for calculating the properties of CO_2 and other gases at high pressures and temperatures, especially in enhanced oil recovery (EOR) and carbon sequestration.

Table 1. Physical and mechanical properties

Property	Value	Unit
Elastic young modulus	1.0	GPa
Poison's ratio	0.25	-
Biot's parameter	1.0	-
Solid phase density	2100	Kg/m^3
Porosity	0.23	-
Intrinsic permeability	4e-14	m^2
Brine compressibility	4e-10	1/Pa
Brine thermal expansion coefficient	6e-4	1/K
Constant injection rate	10	kg/s
Well length	100	m
Residual brine saturation	0.2	-
Residual CO_2 saturation	0.0	-
Entry pressure	10	kPa
Brooks-Corey parameter	2.0	-

The details of this equation are beyond the scope of this paper. The other physical and mechanical properties of the reservoir rock and fluids are assumed as specified in Table 1. The sensitivity analysis was conducted to achieve a balance between computational cost and accuracy in the results. The finite element mesh, with optimized minimum and maximum mesh sizes, was selected as shown in Fig. 2.

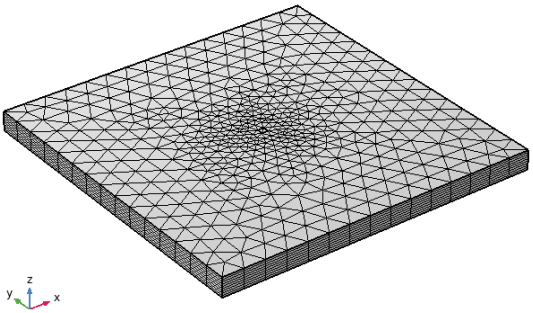

Fig. 2. Finite element mesh for CO_2 injection with vertical well.

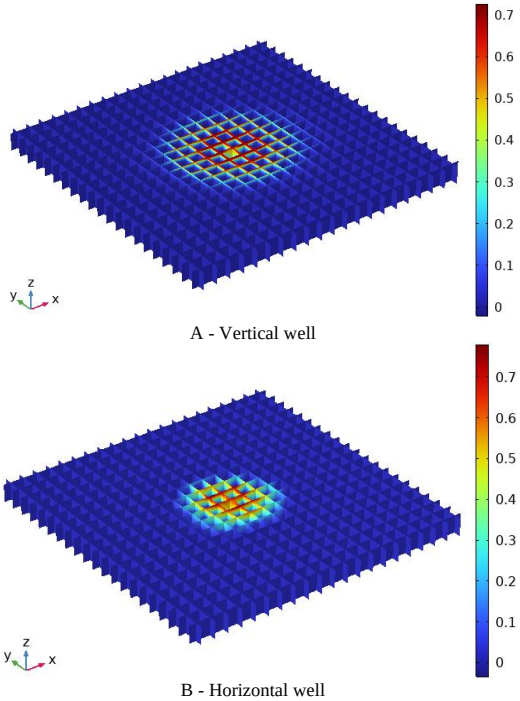

Fig. 3. Contours of CO_2 saturation after 50 years of injection for A) vertical well and B) horizontal well.

4. Results and Discussion

This section presents numerical results and discussions for both vertical and horizontal well conditions. Fig. 3 shows the contour of the distribution of injected CO_2 saturation after 50 years of injection in both vertical and horizontal

wells. It can be observed that, due to its lower density compared to saline water, the injected CO_2 is positioned at higher levels than the saline water. Additionally, comparing the two contours presented in Fig. 3 reveals that, in the case of the vertical well, the CO_2 plume has spread over a wider area compared to the horizontal well, extending at higher levels in the aquifer. This is better illustrated in Fig. 5, which shows the CO_2 saturation after 50 years in a cross-section passing through the center of the aquifer along the x-axis (aligned with the horizontal well and intersecting the vertical well as shown in Fig. 4).

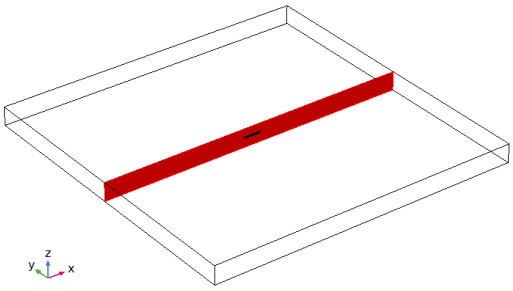

Fig. 4. Definition of the cross section along the x-axis

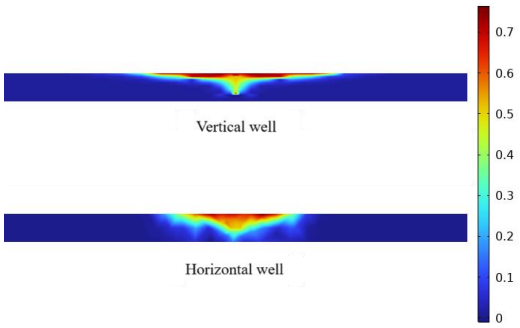

Fig. 5. Comparison of CO_2 saturations at cross section along the x-axis, after 50 years of injection for vertical and horizontal wells.

Fig. 7 illustrates the vertical displacement at the top surface of the aquifer along the line shown in Fig. 6 after 50 years of injection in vertical and horizontal wells. It can be observed that, due to the higher concentration of the CO_2 plume around the horizontal injection well, the uplift at the top surface of the aquifer above the horizontal well is greater than that above the vertical well. However, the spread of uplift over greater distances from the well is more pronounced in the case of the vertical well.

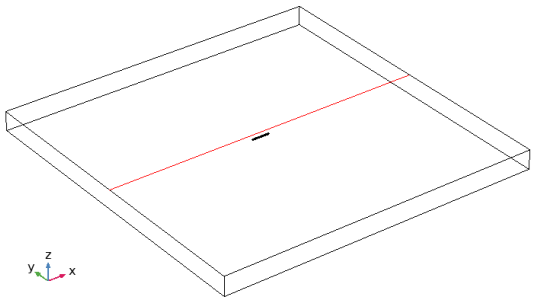

Fig. 6. Definition of the cut line along the x-axis at the top surface of the aquifer above the horizontal or vertical wells.

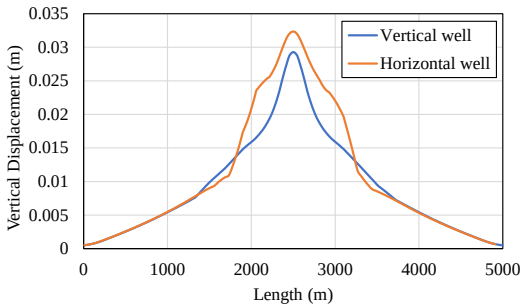

Fig. 7. Vertical displacement at the top surface of the aquifer along the x-axis above the horizontal and vertical wells.

Injected CO_2 disperses and expands within the reservoir due to capillary forces and the density difference between saline water and CO_2. As a result, if the injection ceases, the pressure from the injection gradually decreases, partially offsetting the deformation caused by the injection. To examine this, CO_2 is injected at a constant rate of 10 kg/s up to 20 years, after which the modeling continues to observe subsequent ground displacement changes due to the free diffusion of CO_2 throughout the aquifer. Fig. 8 shows the distribution of injected CO_2 in the aquifer for Case A, with injection over 50 years, and Case B, with injection over 20 years followed by CO_2 diffusion in the aquifer for 30 years. It is observed that in the second case, the injected CO_2 spreads within the aquifer due to capillary and gravitational forces, leading to a reduction in the saturation level around the injection well. This is more clearly seen in Fig. 9, which shows the CO_2 saturation on the cross-section of the aquifer along the x-axis.

Also, as observed in Fig. 10, with the start of injection, upper boundary deformation reaches its maximum within a short period (about 2 years) after the initiation of injection. However, subsequently, due to the dispersion of CO_2 in the aquifer, the uplift amount decreases from its initial maximum value. The reason for this is the sudden increase in aquifer pressure due to injection in the early stages, which later declines as CO_2 spreads to regions farther from the well within the aquifer, thereby reducing the initial pressure and resulting in decreased uplift.

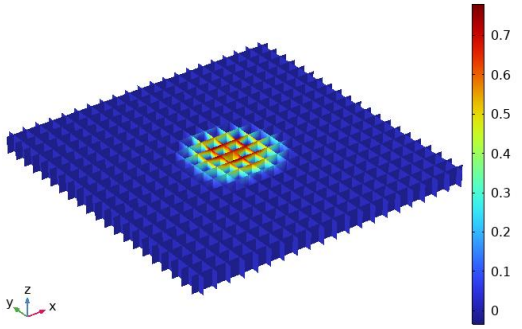

A - Injection for 50 years

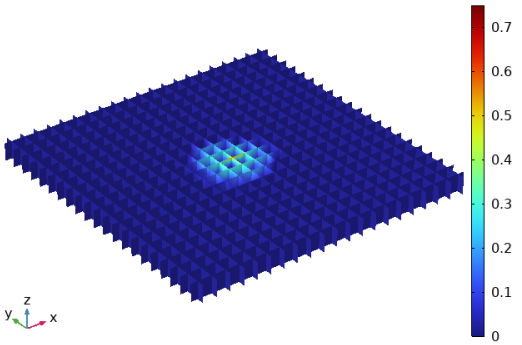

B - Injection for 20 years and spreading of CO_2 for 30 years

Fig. 8. Contours of CO_2 saturation for horizontal well. A) 50 years of injection and B) Injecting for 20 years and spreading of CO_2 for 30 years.

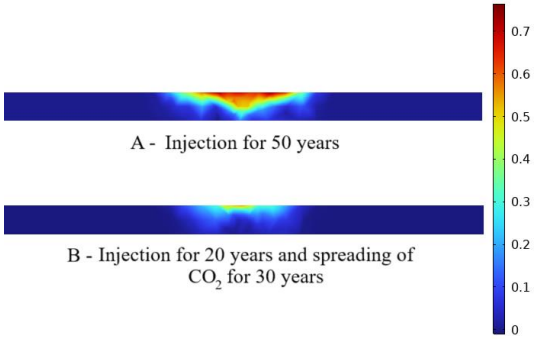

Fig. 9. Comparison of CO_2 saturations at cross section along the x-axis, A) 50 years of injection and B) Injecting for 20 years and spreading of CO_2 for 30 years (horizontal well).

Additionally, Fig. 10 shows that, with the cessation of injection at the 20-year mark, a significant portion of the induced uplift diminishes within a short period; however, a small amount of uplift still remains. The residual uplift in the horizontal well is greater than the residual uplift in the vertical well.

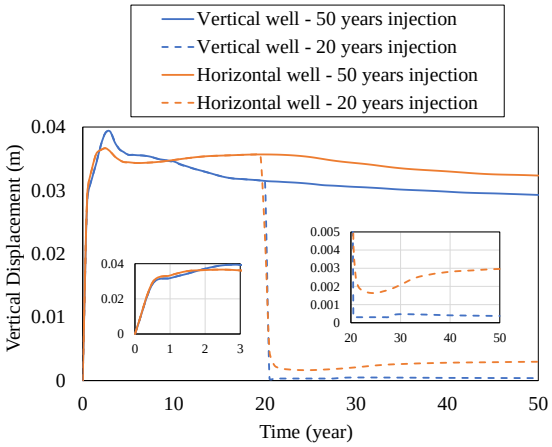

Fig. 10. Time variations of vertical displacement at the point above the center of injection wells.

To investigate the effects of anisotropy in the aquifer's intrinsic permeability on ground deformation, it is assumed that horizontal permeability is 10 times greater than vertical permeability (i.e., horizontal permeability is set to 4×10^{-13} m^2).

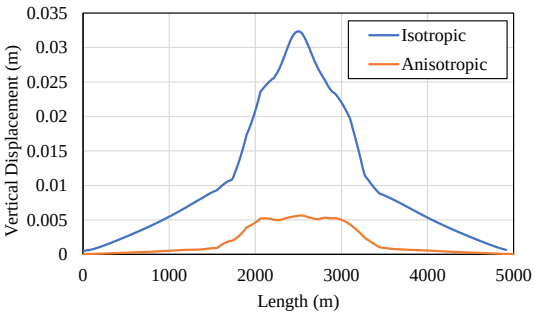

Fig. 11. Vertical displacement at the top surface of aquifer along the x-axis above the horizontal well for isotropic and anisotropic permeability.

As shown in Fig. 11 and Fig. 12, anisotropy in relative permeability, as defined previously, leads to a reduction in the uplift of the upper surface of the aquifer. This is due to the absolute permeability in the horizontal directions being 10 times greater than in the vertical direction, which causes the CO2 plume to spread more laterally, as shown in Fig. 13. Consequently, the pressure induced by CO2 injection is lower than in the isotropic case, resulting in a significant reduction in uplift.

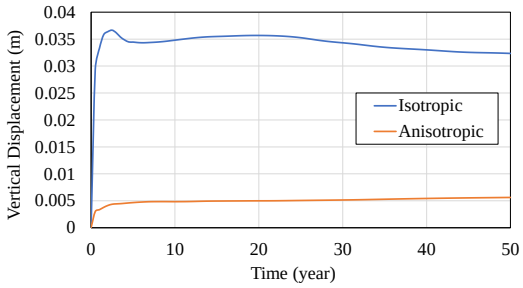

Fig. 12. Time variations of vertical displacement at the point above the center of horizontal well for isotropic and anisotropic permeability.

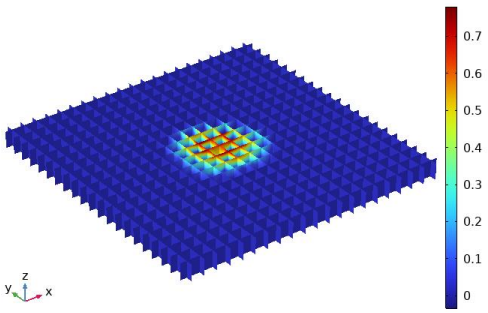

Fig. 13. A – Isotropic permeability

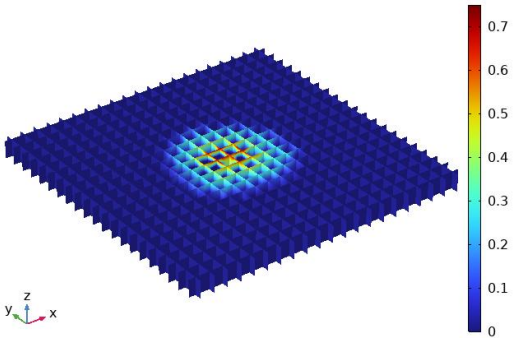

B – Anisotropic permeability

Fig. 14. Contours of CO_2 saturation for horizontal well. A) Isotropic permeability and B) Anisotropic permeability.

5. Conclusions

This study aims to examine the uplift profile of the top surface of a deep saline aquifer layer as a result of CO_2 injection. For this purpose, a 300-meter-thick aquifer layer at a depth of approximately 3000 meters below the ground surface was investigated using the finite element numerical method. Variations in the density and viscosity of the injected supercritical CO_2 were considered as functions of temperature and pressure, and the density and viscosity of saline water were also treated as temperature- and pressure-dependent. Additionally, geothermal temperature variations (constant over time) were included in the model. In analyzing ground uplift at the top surface of the aquifer, both horizontal and vertical well configurations were examined.

The modeling results showed that with a vertical well, the CO_2 plume extended to higher levels and farther regions from the injection well compared to a horizontal well. Consequently, the aquifer surface uplift was greater for the horizontal well than for the vertical well. The impact of injection cessation after a certain period, as well as the spread of injected CO_2 in the aquifer due to capillary and gravitational forces, was also investigated concerning the displacements induced during injection. Furthermore, it was observed that anisotropy in permeability, where the intrinsic horizontal permeability was ten times the vertical permeability, led to a horizontal spread of the CO_2 plume and significantly reduced the aquifer surface uplift. Numerical modeling, incorporating the complexities of the aquifer and the fluids involved, enables accurate engineering predictions and designs.

4. References

[1] Gibbins J, Chalmers H. Carbon capture and storage. Energy Policy 2008;36:4317–22. https://doi.org/10.1016/j.enpol.2008.09.058.

[2] Raza A, Gholami R, Rezaee R, Rasouli V, Rabiei M. Significant aspects of carbon capture and storage – A review. Petroleum 2019;5:335–40. https://doi.org/10.1016/j.petlm.2018.12.007.

[3] Allen DE, Strazisar BR, Soong Y, Hedges SW. Modeling carbon dioxide sequestration in saline aquifers: Significance of elevated pressures and salinities. Fuel Process Technol 2005;86:1569–80. https://doi.org/10.1016/j.fuproc.2005.01.004.

[4] Ang L, Yongming L, Xi C, Zhongyi Z, Yu P. Review of CO2 sequestration mechanism in saline aquifers. Nat Gas Ind B 2022;9:383–93. https://doi.org/10.1016/j.ngib.2022.07.002.

[5] Ringrose PS, Furre AK, Gilfillan SMV, Krevor S, Landroslash M, Leslie R, et al. Storage of Carbon Dioxide in Saline Aquifers: Physicochemical Processes, Key Constraints, and Scale-Up Potential. Annu Rev Chem Biomol Eng 2021;12:471–94. https://doi.org/10.1146/annurev-chembioeng-093020-091447.

[6] Arjomand E, Salimzadeh S, Mow WS, Movassagh A, Kear J. Geomechanical modelling of ground surface deformation induced by CO2 injection at In Salah, Algeria: Three wells, three responses. Int J Greenh Gas Control 2024;132:104034. https://doi.org/10.1016/j.ijggc.2023.104034.

[7] Bjørnarå TI, Bohloli B, Park J. Field-data analysis and hydromechanical modeling of CO2 storage at In Salah, Algeria. Int J Greenh Gas Control 2018;79:61–72. https://doi.org/10.1016/j.ijggc.2018.10.001.

[8] Rutqvist J, Vasco DW, Myer L. Coupled reservoir-geomechanical analysis of CO2 injection and ground deformations at In Salah, Algeria. Int J Greenh Gas Control 2010;4:225–30. https://doi.org/10.1016/j.ijggc.2009.10.017.

[9] Onuma T, Ohkawa S. Detection of surface deformation related with CO2 injection by DInSAR at In Salah, Algeria. Energy Procedia 2009;1:2177–84. https://doi.org/10.1016/j.egypro.2009.01.283.

[10] Shukla R, Ranjith P, Haque A, Choi X. A review of studies on CO2 sequestration and caprock integrity. Fuel 2010;89:2651–64. https://doi.org/10.1016/j.fuel.2010.05.012.

[11] Cheng Y, Liu W, Xu T, Zhang Y, Zhang X, Xing Y, et al. Seismicity induced by geological CO2 storage: A review. Earth-Science Rev 2023;239:104369. https://doi.org/10.1016/j.earscirev.2023.104369.

[12] Nicol A, Carne R, Gerstenberger M, Christophersen A. Induced seismicity and its implications for CO2 storage risk. Energy Procedia 2011;4:3699–706. https://doi.org/10.1016/j.egypro.2011.02.302.

[13] Fang Y, Baojun B, Dazhen T, Dunn-Norman S, Wronkiewicz D. Characteristics of CO2 sequestration in saline aquifers. Pet Sci 2010;7:83–92. https://doi.org/10.1007/s12182-010-0010-3.

[14] Massarweh O, Abushaikha AS. CO2 sequestration in subsurface geological formations: A review of trapping mechanisms and monitoring techniques. Earth-Science Rev 2024;253:104793. https://doi.org/10.1016/j.earscirev.2024.104793.

[15] Ali M, Jha NK, Pal N, Keshavarz A, Hoteit H, Sarmadivaleh M. Recent advances in carbon dioxide geological storage, experimental procedures, influencing parameters, and future outlook. Earth-Science Rev 2022;225:103895. https://doi.org/10.1016/j.earscirev.2021.103895.

[16] Preisig M, Prévost JH. Coupled multi-phase thermo-poromechanical effects. Case study: CO2 injection at In Salah, Algeria. Int J Greenh Gas Control 2011;5:1055–64. https://doi.org/10.1016/j.ijggc.2010.12.006.

[17] Iranmanesh MA, Pak A, Samimi S. Non-isothermal simulation of the behavior of unsaturated soils using a novel EFG-based three dimensional model. Comput Geotech 2018;99:93–103. https://doi.org/10.1016/j.compgeo.2018.02.024.

[18] Li C, Barès P, Laloui L. A hydromechanical approach to assess CO2 injection-induced surface uplift and caprock deflection. Geomech Energy Environ 2015;4:51–60. https://doi.org/10.1016/j.gete.2015.06.002.

[19] Naddafnia M, Pak A, Iranmanesh MA, Tourei A. An Element Free Galerkin Simulation of - CO2 Sequestration in Nonhomogeneous Saline Aquifers. Int J Environ Res 2025. https://doi.org/10.1007/s41742-024-00692-5.

[20] Lewis RW, Schrefler BA. The Finite Element Method in the Static and Dynamic Deformation and Consolidation of Porous Media. Chichester: Wiley; 1998. https://doi.org/10.1137/1031039.

[21] Brooks RH, Corey AT. Hydraulic properties of porous media. Color State Univ Hydrol Pap Fort Collins, CO State Univ 1964.

[22] Brooks RH, Corey AT. Properties of Porous Media Affecting Fluid Flow. J Irrig Drain Div 1966;92:61–88. https://doi.org/10.1061/jrcea4.0000425.

[23] Peng DY, Robinson DB. A New Two-Constant Equation of State. Ind Eng Chem Fundam 1976;15:59–64. https://doi.org/10.1021/i160057a011.